SERIAL RESISTANCE ANALYSIS WITH THE SHADED LUMINESCENCE TECHNIQUE

J.-M. Wagner, J. Carstensen, A. Berhane, A. Schütt, and H. Föll
Institute for General Materials Science, Faculty of Engineering, Christian-Albrechts-University of Kiel,
Kaiserstr. 2, 24143 Kiel, Germany, email: jwa@tf.uni-kiel.de, Phone: (+49) 431 880 6180, Fax: (+49) 431 880 6178

ABSTRACT: Guided by the interpretation of CELLO open circuit voltage measurements a model for calculating local serial resistance maps $R_{ser}(x, y)$ from luminescence images is introduced which uses the Taylor series in linear order of the extracted current starting from open circuit condition. This approach is in strong contrast to the model of independent diodes frequently used for obtaining $R_{ser}(x, y)$ maps from luminescence data. An optimal mode when just using two luminescence maps is introduced, together with two additional variants, one which just needs two pure electroluminescence maps and one which is completely contactless. Especially the contactless "shaded luminescence" mode has a high potential to be used as inline measurement technique. On several examples the results of the three modes are compared. Limitations and possible improvements in data evaluation for the two additional modes are discussed. For typical mc-Si solar cells all three modes give similar quantitative results.

Keywords: characterization, serial resistance, luminescence, EL, PL

1 INTRODUCTION

The ongoing efforts for improving the grid design and contacting concepts like selective emitter, EWT, or MWT demonstrate the importance of reducing ohmic losses without increasing current losses. Future production lines will need a fast and reliable inline check of local serial resistance and most probably luminescence imaging will be the optimal tool for this as indicated by the continuously increasing number of papers on this topic.

Assuming a perfect grid leading to a perfect equipotential layer luminescence images would not differ for three different types of current injection: i) homogeneous illumination, ii) inhomogeneous illumination; iii) injection of current via the grid. Any difference in the injected current profile instantly would be leveled out by lateral current flow without any ohmic losses. So differences in the luminescence images for the three different current injection types on real solar cells with serial resistance losses just reflect the local serial resistance distribution. CELLO voltage measurements on a large variety of solar cell types (actually all which have been measured in the last years) indicate that for quite large currents still the grid and emitter provide for a quasi equipotential layer, only leading to a linear variation of the potential across the area of the solar cell. This linear relationship can be checked for any serial resistance map and thus serves as a consistency check for the whole analysis. The consequences of a nearly perfect grid have been verified from luminescence data as discussed in this paper for three different modes for serial resistance analysis combining the three different current injection types. For instance, combining standard open circuit luminescence imaging (homogeneous illumination) with open circuit images when shading reasonable areas of the solar cell (inhomogeneous illumination), i.e. being completely contactless, allows a fully quantitative local serial resistance analysis on a large variety of standard mono- and multicrystalline solar cells.

2 MODELING OF SERIAL RESISTANCES

Starting from the voltage distribution at open circuit condition $U_0(x, y)$, the voltage distribution when applying a current I is in linear order given by

$$U(x, y, I) = U_0(x, y) + R(x, y)\, I \,. \tag{1}$$

With respect to a probing electrode (somewhere on a main bus bar) the full lateral ohmic voltage loss can be calculated from the path integral

$$\tilde{U}_{ser}(x, y, I) = -\int_{\vec{r}_e}^{\vec{r}} \rho\, \vec{j}\, d\vec{r} = U(x_e, y_e, I) - U(x, y, I) \,. \tag{2}$$

Here ρ is the specific resistance and $\vec{j}$ the local current density along the path. Knowing the voltage distribution of course the ohmic voltage loss can just be calculated from the potential difference and no knowledge about the local current distribution is necessary. This is important to note because lateral currents $\vec{j}_{oc}$ even under open circuit condition are induced by inhomogeneous solar cell parameters like e.g. life time τ or diode current densities j_0. The additional local ohmic voltage losses induced by the externally applied current I can easily be calculated in linear order by combining Eq. (1) and Eq. (2):

$$U_{ser}(x, y, I) = \left[R(x_e, y_e) - R(x, y)\right] I =: R_{ser}(x, y)\, I \,. \tag{3}$$

This definition allows to rewrite Eq. (1) as

$$U(x, y, I) = U_0(x, y) + \left[R(x_e, y_e) - R_{ser}(x, y)\right] I \;, \tag{4}$$

which is a more familiar representation of the serial resistance losses and emphasizes that an external current flow not just leads to ohmic losses but of course also to an offset in the applied potential.

The above definition of a local serial resistance is equivalent to those standard models for analyzing photoluminescence which assume a spatially constant, average photocurrent density for calculating local serial resistances (cf. [1–3]). In this case $R_{ser}(x, y)\times A$ (with the total area A of the solar cell) is plotted and the dimension is Ωcm^2, but this is an unnecessary complication.

Basically, the difference in all procedures to analyze the local serial resistance distribution is the choice of measurement conditions and computational tricks to eliminate the unknown distribution of

$$U_0(x_e, y_e) - U_0(x, y), \tag{5}$$

but one should be aware that all procedures including that proposed in this paper do not analyze all ohmic losses.

To apply Eq. (3) correctly, the linearization in Eq. (1) must hold. Since the metal grid and the emitter layer show essentially pure ohmic resistances the main source for nonlinearities is the p-n junction with the diode-like IV characteristic; a second source for nonlinear behavior may be injection-level-dependent bulk recombination. Staying well in the high injection regime, the solar cell's IV curve can be well described by

$$I(U(x_e, y_e)) = I_0 \exp\left(\frac{q\left[U_0(x_e, y_e) + R(x_e, y_e)I\right]}{kT}\right) - I_{\mathrm{Ph}} . \tag{6}$$

Here we used Eq. (1) to express the standard representation of the IV curve using the distribution functions introduced above. The least nonlinear effects occurring for varying the external current should be expected when the exponential factor in Eq. (6) does not change, i.e. when

$$I(U(x_e, y_e)) + I_{\mathrm{Ph}} = const \ , \tag{7}$$

which means to adjust the global illumination and thus to change I_{Ph} by exactly the amount by which the extracted current I varies.

Two further results for the linearized function $R(x, y)$ in Eq. (1) are described e.g. in [4–6]. They hold for conditions which are fulfilled for nearly all solar cells and have been verified by CELLO measurements on several hundred cells in the last years. We state them because they allow a deeper insight into the photoluminescence measurements and because they can be easily checked by the luminescence measurements presented here.

The first statement quantifies a well-known effect, that the serial resistance decreases in forward direction because a part of the lateral current is short circuited by the p-n junction:

$$\frac{1}{\left\langle R_{\mathrm{ser}}(x,y)\right\rangle} = \frac{1}{\left\langle R_{\mathrm{ser},\infty}(x,y)\right\rangle} + \left\langle \frac{1}{R_D} \right\rangle . \tag{8}$$

Here, the angle brackets indicate the average value taken over the respective map, and

$$\left\langle \frac{1}{R_D} \right\rangle := \frac{\partial I_D}{\partial U_D} = \frac{I_0 q}{kT} \exp\left(\frac{qU_0(x_e, y_e)}{kT}\right), \tag{9}$$

which can easily be extracted from Suns-U_{oc} measurements. Please note that here $U_0(x_e, y_e) = U_{\mathrm{oc}}$. $R_{\mathrm{ser},\infty}(x, y)$ is the serial resistance distribution for infinite diode resistance. As stated before, the photoluminescence measurements will be performed in the high injection regime. Therefore Eq. (8) is important because it holds in linear order and cannot even be neglected for small currents I.

The second result is related to the histogram $H(R)$ calculated from the map of $R(x, y)$. Defining the integral

$$N(R) := \int_{R_{\min}}^{R} H(R')\,dR' \tag{10}$$

the function $\alpha(R) := N(R) / N(R_{\max})$ respectively the inverse function $R(\alpha)$ will be a straight line.

The local luminescence intensity can be well described by [1]

$$C(x,y) \exp\left(\frac{q\left[U_0(x,y) + R(x,y)I\right]}{kT}\right) ; \tag{11}$$

here we already replaced the voltage distribution $U(x, y, I)$ by the linearized version of Eq. (1). $C(x, y)$ depends mainly on the local diode current density j_0 and on the local life time τ. Fulfilling Eq. (7) when varying the external current I fixes not only the integral diode characteristics but also, according to Eq. (9), the average diode resistance – which, according to Eq. (8), fixes the average serial resistance as well. Since the sum of the overall injected current stays constant, least variation in a possibly injection-level-dependent bulk life time and in $U_0(x, y)$ [see Eq. (1)] can be expected. Finally the linear relation for $R(\alpha)$ implies that the average luminescence intensity does not change when the global illumination is tuned to fulfill condition (7), which allows to fulfill Eq. (7) without measuring currents and thus to be applied in a situation where the solar cell is not contacted at all or where short circuit currents are difficult to be measured due to serial resistance losses.

The most accurate serial resistance measurements based on only two luminescence images thus can be performed using the following procedure:

a) Choose a global illumination to stay in high injection, extract a current I_1 e.g. by connecting back and front of the solar cell with an appropriate resistor. Take a luminescence map $M_1(x, y)$ and check for the average $\langle M_1 \rangle$.
b) Change the resistance. Measure a luminescence map $M_2(x, y)$ and tune the global illumination until $\langle M_2 \rangle = \langle M_1 \rangle$ holds. This may seem to be a time consuming job, but taking into account Eq. (7) for a known type of solar cells this typically takes one or two trials. (Actually an error of 5% to 10% in the average intensities already shows quite good results.) For this condition measure the second current I_2.
c) Take the logarithm of both maps and subtract the first from the second. Multiply the difference by $kT/(q\,\Delta I)$ (with $\Delta I = I_2 - I_1$) to get a map $R(x, y)$.
d) Find the maximum $R_{\max}$ of $R(x, y)$. Here some random noise-induced points should be neglected which are the points with the smallest ohmic losses and thus are near the main bus bars, i.e. $R_{\max} = R(x_e, y_e)$. Calculate $R_{\mathrm{ser}}(x, y) = R_{\max} - R(x, y)$.
e) In addition the histogram data $H(R)$ of $R(x, y)$ can be integrated using Eq. (10) to check for a straight line for $R(\alpha)$.

This procedure can be simplified by taking $I_2 = 0$, i.e. one of the two maps can just be an open circuit map.

As a modification, one can also use two electroluminescence maps taken for different currents; in this case condition (7) is not fulfilled which gives rise to some minor artifacts but still results in astonishingly good maps.

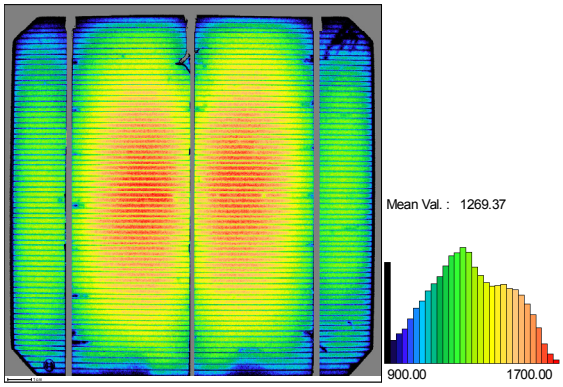

a)

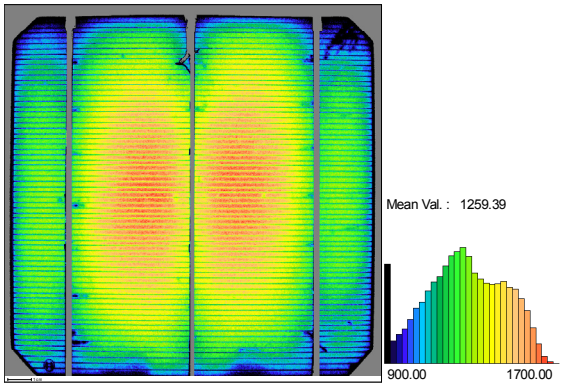

b)

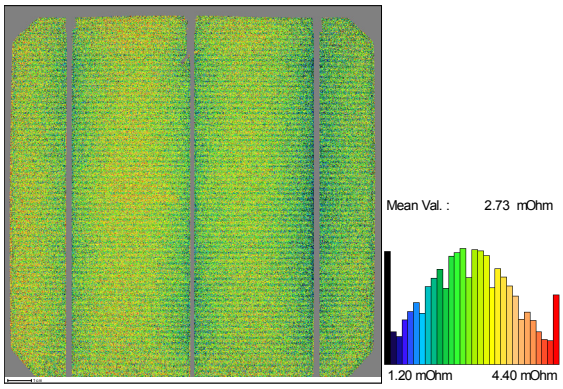

c)

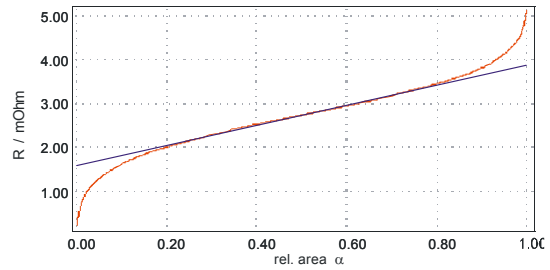

d)

Fig. 1: Luminescence maps for mono-Si solar cell a) with 0.88 A current extraction; b) corresponding open circuit map with same luminescence intensity. c) Calculated R_{ser} map; d) straight line using Eq. (10) extracted from the histogram in c).

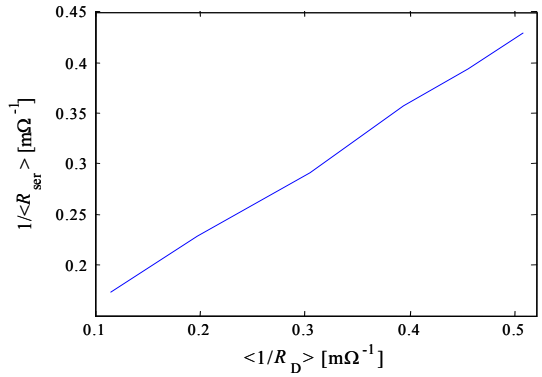

Fig. 2: $1/\langle R_{ser}\rangle$ vs. $\langle 1/R_D\rangle$ extracted from maps like Fig. 1c and Suns-U_{oc} measurements using Eq. (9).

Guided by Eq. (11), recombination losses and ohmic losses can be separated from the two electroluminescence maps by multiplying e.g. the first luminescence map $M_1(x, y)$ by

$$\exp\left(\frac{qR_{ser}(x,y)I_1}{kT}\right), \qquad (12)$$

which without illumination allows to generate maps reflecting many features of open circuit maps.

In a third approach the lateral current flow is induced by shading certain areas of the solar cell and combining these maps with open circuit maps; this approach has been patented [7] because it allows a completely contactless analysis of serial resistance losses. In this contribution all three modes are applied to three solar cells (mono-Si, mc-Si, mc-Si with emitter contact problems) to demonstrate the applicability and the consistency of this approach.

3 EXPERIMENTAL RESULTS AND DISCUSSION

All measurements have been performed using a home-made water-cooled LED array providing a very homogeneous illumination of solar cell (size up to 15.6 cm × 15.6 cm) with intensities up to 3 suns. All images have been taken with an integration time of 5 s (mono-Si cell) or 10 s (mc-Si cells) using a Si-based CCD camera with Peltier cooling (Sensicam, PCO imaging). Much more sensitive cameras are available so that all images could easily be measured in less than 1 sec, allowing all three presented modes to be in-line compatible. The first results will be presented for a 15.6 cm × 15.6 cm mono-Si cell. Fig. 1 shows an example for the photoluminescence maps, using the procedure discussed above for extracting a current of 0.88 A (Fig. 1a), open circuit map U_{oc} = 624 mV (Fig. 1b), the resulting R_{ser} map (Fig. 1c), and the straight line extracted from the corresponding $R(x, y)$ distribution (Fig. 1d). By purpose we have chosen a quite small external current to demonstrate that although the map is rather noisy, a very good straight line is found. The reason for this is that two integration procedures which are well known to reduce noise are applied for a) calculating the histogram and b) calculating $N(R)$ according to Eq. (10).

From Suns-U_{oc} measurements, $I_0 = 1.59\times10^{-9}$ A and q/kT = 1 / (27.56 meV) were found, allowing to calculate the average inverse diode resistance according to Eq. (9). Repeating the serial resistance analysis for several values

of U_{oc} and plotting $1/\langle R_{ser}\rangle$ vs. $\langle 1/R_D\rangle$ a straight line is found as shown in Fig. 2, which is in good agreement with the theoretically expected relation, Eq. (8).

Although often checked by CELLO measurements, still the opinion is widespread that there exists only one serial resistance which describes the ohmic behavior along the whole IV curve. This is just not true. Other groups state that reliable serial resistance analysis can only be performed not much above the maximum power point. This is correct to some extent. For voltages around that point and below, the diode resistance is much larger than the serial resistance and a constant serial resistance of $\langle R_{ser,\infty}(x, y)\rangle$ is found. But Eq. (8) allows a quantitative correction of serial resistance data even at higher voltages as illustrated by the straight line in Fig. 2 and by further results discussed in this contribution. This is interesting e.g. because measurements at high illumination intensities show a strongly reduced noise level and thus facilitate short measurement times while still obtaining correct local as well as global serial resistance data by applying Eq. (8).

For the same mono-Si solar cell electroluminescence measurements with two different currents of I_1 = 7 A and I_2 = 3 A have been performed (Fig. 3a and 3b) and analyzed using the same approach. Quite obviously a very good serial resistance map can be generated as shown in Fig. 3c.

By multiplying the first luminescence map $M_1(x, y)$ with the factor defined in Eq. (12) nearly all serial resistance effects can be eliminated to generate a map in Fig. 3d which reflects many features of the open circuit map in Fig. 1a.

The last example presented for the mono-Si cell demonstrates that the procedure can be implemented as a completely contactless mode. Fig. 4a shows an open circuit photoluminescence map where the missing parts of the solar cell have been completely shaded against the global illumination. Figure 4b shows the same result shading the complementary part of the cell. Combining both maps in Fig. 4c much reflects the feature of Fig. 1a where current has been extracted from the cell via the grid. Very similar lateral current flow pattern can be generated by shading appropriate areas. Figure 4d shows the standard open circuit map where the global illumination has been tuned to get the same average luminescence intensity as in Fig. 4c. The lateral current flow can be estimated quite correctly from the difference in the global illumination intensity for Fig. 4c and 4d by applying Eq. (7). Following the standard approach the serial resistance map in Fig. 4e has been calculated which again reveals many features of Fig. 1c. There are some systematic differences between the maps in Figs. 1c, 3c, and 4e. They can be understood qualitatively and quantitatively from Eq. (8); a further discussion will be given in a separate publication.

The same set of three measurements has been repeated on a 15.6 cm × 15.6 cm sized mc-Si cell and the results are summarized in Fig. 5 to Fig. 7. Although for this solar cell the lateral variation of the bulk recombination is much larger all three modes allow a consistent analysis of the local serial resistances as can be checked from comparing Figs. 5c, 6c, and 7c. Taking into account Eq. (9) the differences in the average values for the local serial resistances can be well understood from the different amounts of injected charges especially into the right part of the cell for the three modes.

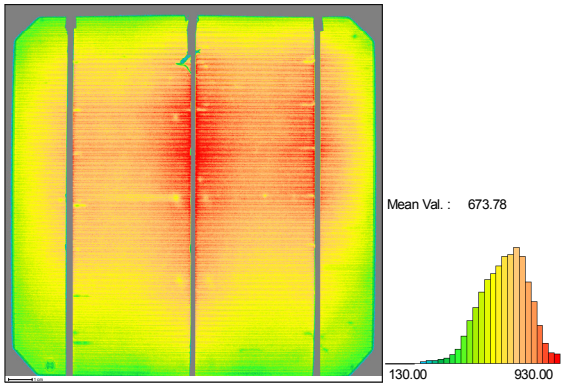

a)

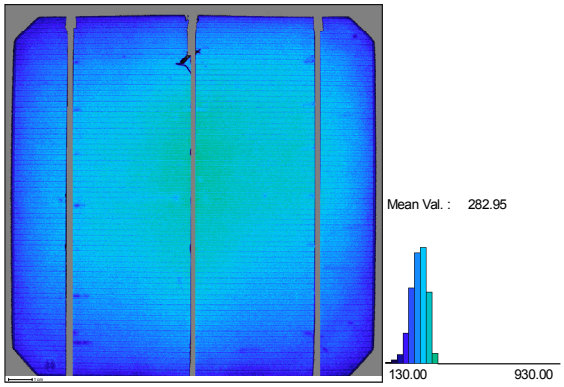

b)

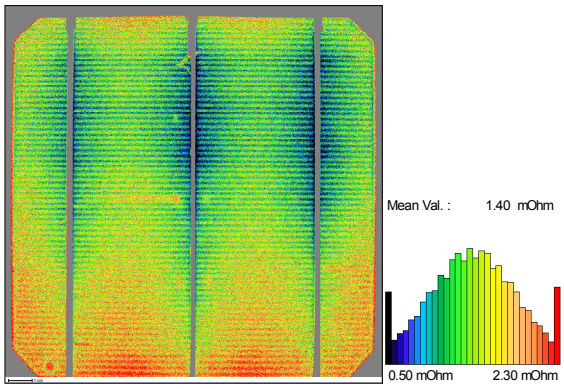

c)

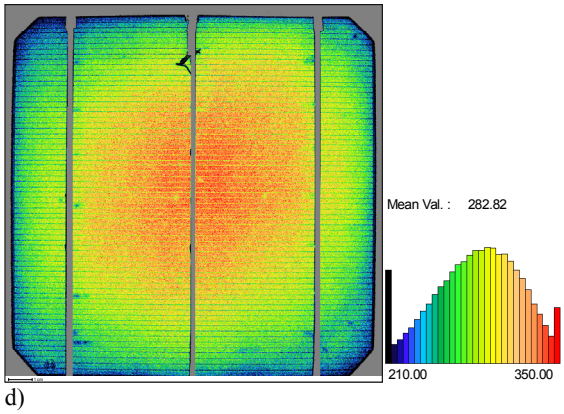

d)

Fig. 3: Pure electroluminescence maps of the solar cell shown in Fig. 1: a) with 7 A b) with 3 A; c) calculated R_{ser} map; d) open-circuit-like map calculated from map a) by multiplying with the factor defined in Eq. (12).

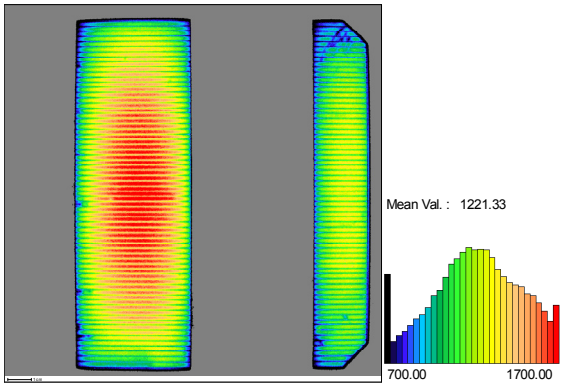

a)

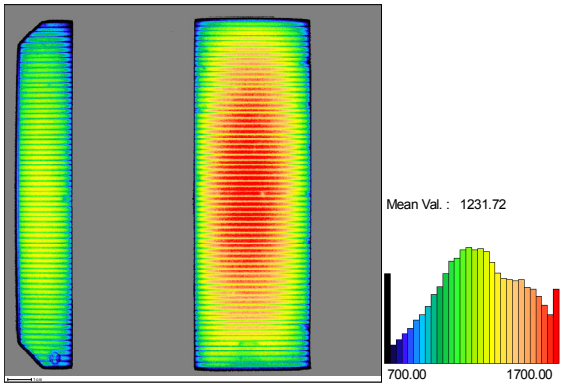

b)

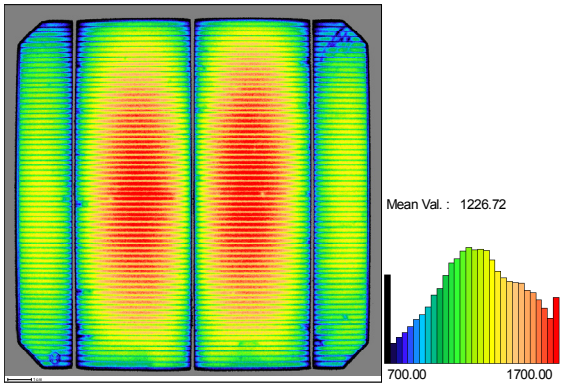

c)

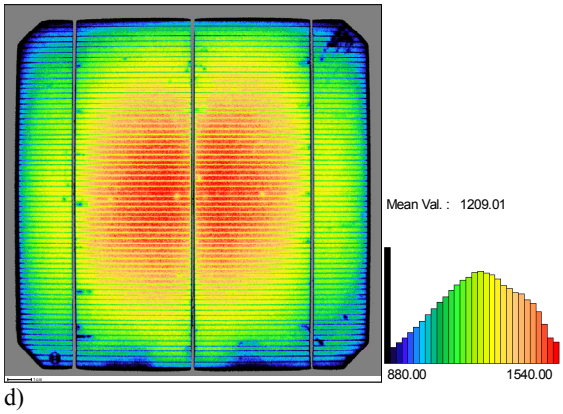

d)

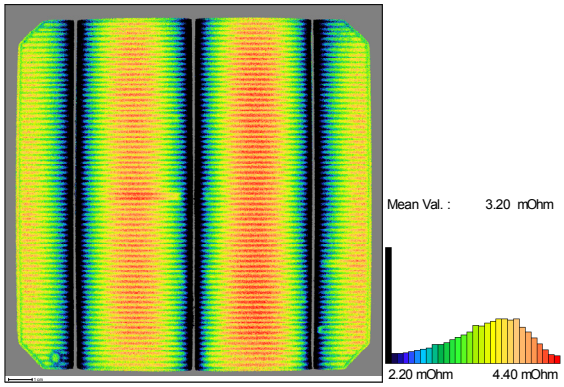

e)

Fig. 4: "Shaded luminescence" (mono-Si cell as before). Open circuit luminescence maps: a), b) with shading complementary parts of the cell; c) combination of a) and b); d) no shading. e) R_{ser} map calculated from c) and d).

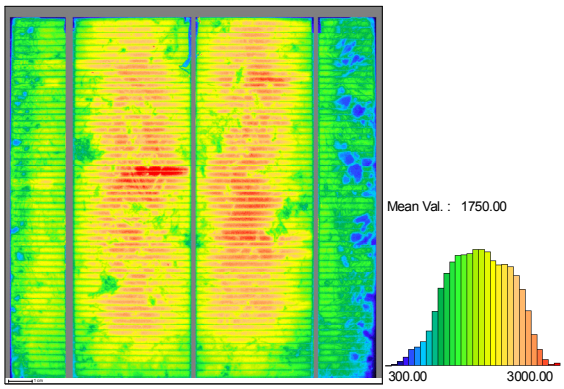

a)

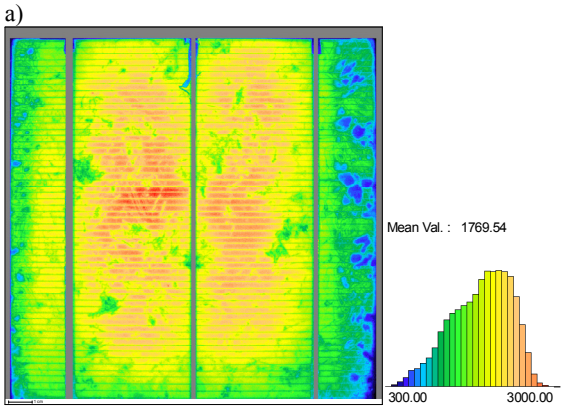

b)

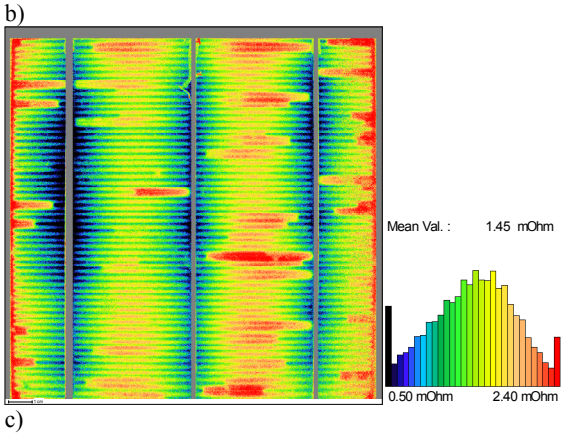

c)

Fig. 5: Luminescence maps for a mc-Si solar cell: a) with 3.7 A current extraction; b) corresponding open circuit with same intensity. c) Calculated R_{ser} map.

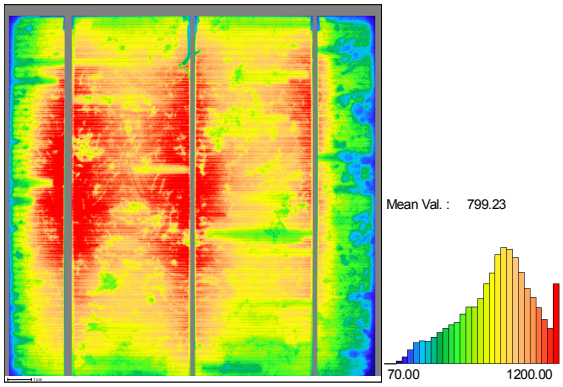

a)

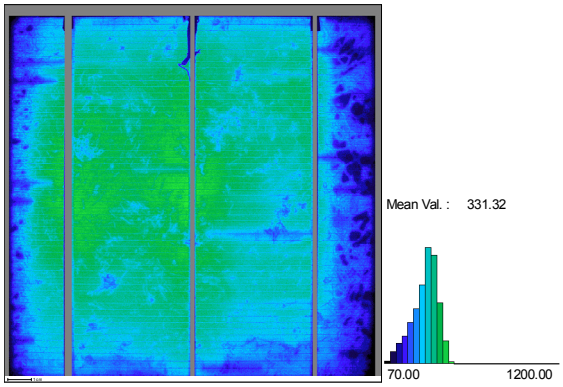

b)

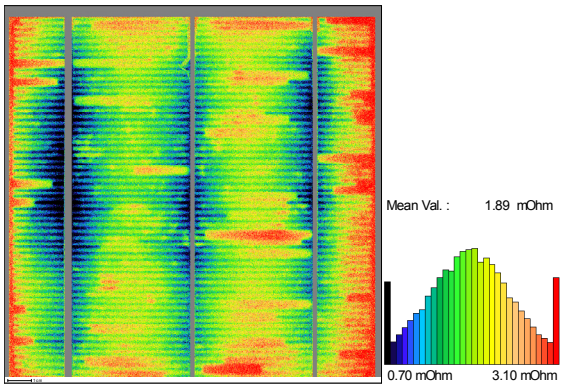

c)

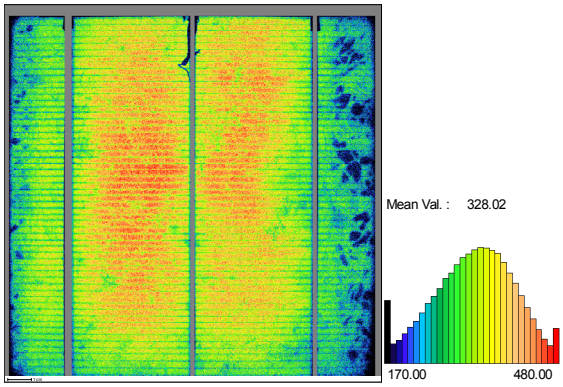

d)

Fig. 6: Pure electroluminescence maps for the same mc-Si solar cell as in Fig. 5: a) with 7 A, b) with 3 A; c) calculated R_{ser} map; d) open-circuit-like map calculated from map a) multiplying the factor defined in Eq. (12).

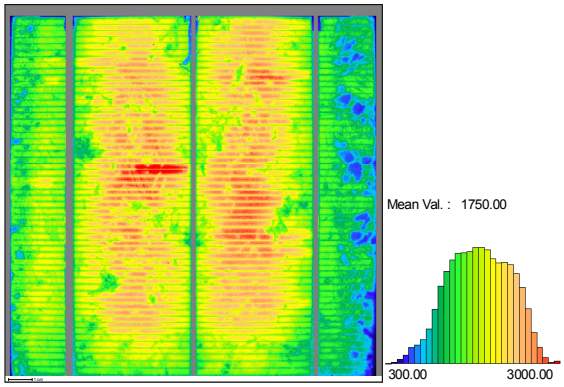

a)

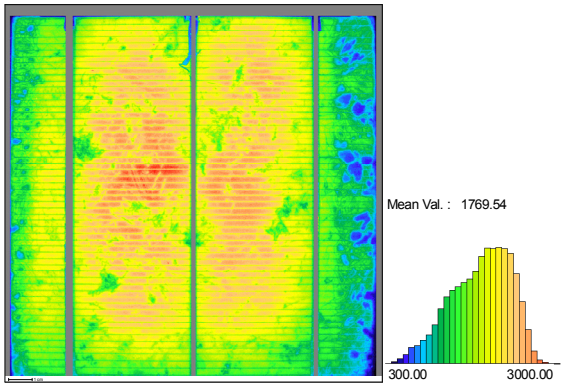

b)

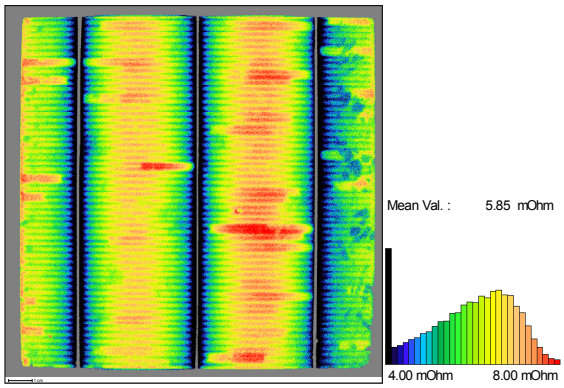

c)

Fig. 7: "Shaded luminescence" for the mc-Si cell of Figs. 5 and 6. a) Combined shaded luminescence map (like Fig. 4c); b) corresponding open circuit map with same luminescence intensity; c) R_{ser} map calculated from maps in a) and b).

As explained in the theory part the first mode was optimized to get the most homogeneous injection across the solar cell and between the different maps. Obviously this is true for this example. So Fig. 5c is the most reliable serial resistance map and indeed shows least (nearly no) artifacts related to local recombination. Although both electroluminescence maps in Fig. 6a and 6b show strong effects of the broken grid fingers, these effects could be completely eliminated in Fig. 6d which shows a remarkably good resemblance to the open circuit maps in Fig. 5b and Fig. 7b. This of course allows a correct analysis of recombination processes just from electroluminescence measurements.

Optimized procedures to get better results even for inhomogeneous injection condition are under way by measuring several open circuit maps at different injection conditions and using for each region the appropriate map with the correct injection condition (similar to the procedure proposed in [2]). In the example of Figs. 5–7 the shaded luminescence mode showed the largest artifacts, although still not a bad result. But e.g. for a solar cell with large areas of severe contact resistance problems between grid fingers and emitter, shown in Fig. 8, the pure electroluminescence mode underestimates the contact resistance problems (Fig. 8b) because the injection into the regions with bad contacts is much smaller, while it is no problem to generate charges in these regions by illumination.

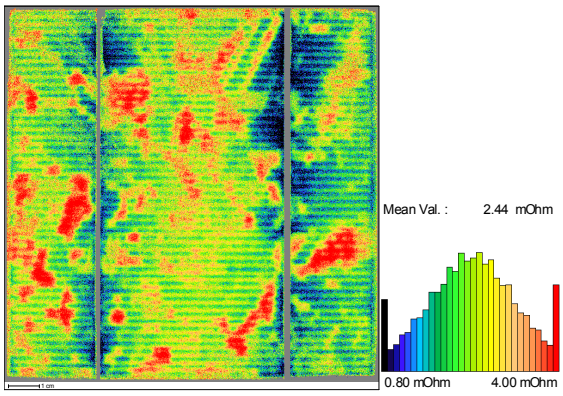

a)

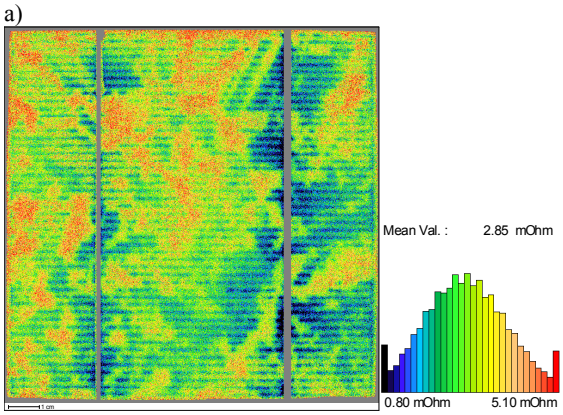

b)

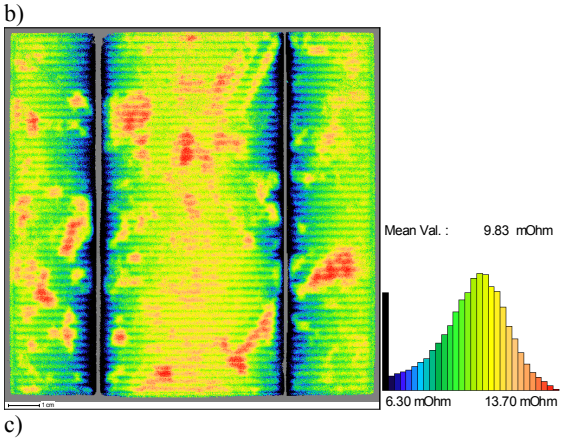

c)

Fig. 8: Series resistance maps of a mc-Si solar cell having many areas with increased contact resistance, determined by the three different measurement modes. a) PL with current extraction (here: 2.2 A) and under open circuit condition; b) EL with 6 A and 4 A; c) "shaded luminescence".

4 SUMMARY

A model has been presented which allows to calculate serial resistance maps from two luminescence maps with different current extraction. Three different inline compatible modes for inducing lateral currents have been tested which allow to obtain similar quantitative results, of which the shaded luminescence approach is most attractive for inline monitoring since it allows a completely contactless analysis.

5 ACKNOWLEDGEMENTS

We like to thank the Fraunhofer ISE in Gelsenkirchen for the supply of solar cells with various firing conditions.

6 REFERENCES

[1] T. Trupke, E. Pink, R.A. Bardos, and M.D. Abbott, *Appl. Phys. Lett.* **90**, 093506 (2007).

[2] H. Kampwerth, T. Trupke, J.W. Weber, and Y. Augarten, *Appl. Phys. Lett.* **93**, 202102 (2008).

[3] M. Glatthaar, J. Haunschild, M. Kasemann, J. Giesecke, W. Warta, and S. Rein, *Phys. Status Solidi RRL* **4**, 13 (2010).

[4] J. Carstensen, A. Schütt, and H. Föll, in *Proc. 22nd European Photovoltaic Solar Energy Conference*, 1CV.1.34, Milan (2007).

[5] J. Carstensen, A. Schütt, and H. Föll, in *Proc. 23rd European Photovoltaic Solar Energy Conference*, 1CV.1.38, Valencia (2008).

[6] J. Carstensen, A. Abdollahinia, A. Schütt, and H. Föll, in *Proc. 24th European Photovoltaic Solar Energy Conference*, 1CV.4.33, Hamburg (2009).

[7] W. Warta, M. Kasemann, J. Carstensen, A. Schütt, and H. Föll, *Deutsche Patentanmeldung* 10 2008 010 672.0-52, 1 (2008).